Outwardly Propagating Spherical Flame with Cellular Instabilities and Laminar Burning Velocities in Methane/ethylene/air Premixed Flames.

K. H. Van*, H. J. Kim*, J. Park*†, Oh. Boong Kwon*,Dae. Keun Lee**, Seung Gon Kim**, Young Tae Guahk**, Dong-Soon Noh**, S. H. Chung***

* Dept. of Mechanical Engineering, Pukyong National University, Busan, Korea.

** Advanced Combustion Lab, Korea Institute of Energy Research, Daejeon, Korea.

*** Clean Combustion Research Center, King Abdullah University of Science and Technology, Saudi Arabia

1. Introduction

Lean-burn which refers to the burning of lean fuel with excess of air must be bright technology to solve the problems on serious depletion fossil fuel and environmental regulation of air pollutant emissions (low nitric oxide emissions) in the current situation. Natural gas with methane being its major component, has been widely used to solve global-warning problem. However, there still remain some assignment for solution such as fragmentary heat losses to reduce laminar burning velocities and thermal efficiency as well as poor lean-burn capability [1]. In this situation, the comprehensive study has been conducted to solve these problems via using blended fuels on methane or hydrogen [2]. In interaction between lean premixed methane-air and hydrogen-air flames, lean flammable limits were extended significantly while the extinction behaviors were influenced complicatedly by the existence of hydrogen, e.g. preferential diffusion of H and H_2 as well as complicated chemical effects of sharing the radicals such as H, O, and OH on extinction behavior [2]. In CH_4/H_2-air laminar premixed flames, lean flammable limit was extended greatly with enrichment of H_2, resulting in significant reduction of NO formation. The effects of additional reformate gas reduced NO formation greatly [3].

Ethylene is the primary olefin feedstock of the modern organic chemical industry and is derived massively in the United States from the advanced extraction technology with steam cracking [4]. Also, ethylene as a key intermediate in the oxidation of higher alkanes has some merits: ignition temperature is lower than that of methane. In this situation, some research efforts have been devoted to grasp fundamental combustion characteristics in ethylene flames, e.g. ignition characteristics [5] and unstretched laminar flame speed [6]. However, those in CH_4/H_2-air flames, have been seldom found in the literature. Considering the feasibility of using methane/ethylene mixtures as a fuel to secure the fuel flexibility particularly in gas turbine combustor, it may be required to extensively study fundamental combustion characteristics in CH_4/H_2-air

Correspondence to: jeongpark@pknu.ac.kr

flames. In the present study, experimental study was conducted to investigate unstretched laminar burning velocities, and cellular instabilities by varying fuel composition at room temperature and elevated pressure (up to 4 atm) in outwardly propagating spherical CH_4/C_2H_4-air premixed flames.

2. Experimental Facility

In the present study, the experiments were conducted in stainless, cylindrical constant-volume chamber with 200 and 220 mm in an inside diameter and a length as shown schematically in Fig. 1. Two quartz windows with 100 mm in diameter and 40 mm in thickness were mounted oppositely on both flat sides of the chamber for visual access. Two movable, opposed tungsten electrodes diameter were connected to a high voltage source to ignite the mixture at the center of the chamber. Purity of methane and ethylene is 99.99 % and air with that of 99.95 %, respectively. Fuels and air were supplied to the inside chamber such that the partial pressure of each reactant was adjusted by a pressure transmitter to achieve the desired initial pressure. To ensure complete mixing of supplied reactants to the chamber and their quiescence, the experiments was conducted after 15 minutes elapsed. After the flame propagation was completed, the chamber was ventilated to the laboratory exhaust system and purged with an air compressor to get rid of condensed water for the next experiment. The outwardly propagating spherical flame was visualized using a Schlieren photography with a xenon light source and a pair of concave mirrors, and taken with framing rate of 10,000 fps by a high –speed camera. The edge of the flame front was determined by a Matlab-based code and then converted to flame radius. Operating the high-speed camera and measuring the instantaneous chamber pressure were triggered by the signal of the signal of the spark ignition source.

3. Results and discussion

The error in S_u^0 due to discrepancies in equivalence ratio, mixture preparation, buoyancy, ignition transition, radiation-induced reduction and effect of confinement [7, 8]. Resultantly, to reduce the discrepancy of uncertainty on flame speed, it may be required to determine the range of flame radius for extrapolation model. Three extrapolation linear and nonlinear models (LM, NM I, and NM II) in the followings were investigated:

$$LM: \; S_b^0 - S_b = L_b K \tag{1}$$

$$NM\text{ I}: S_b = S_b^0 - S_b^0 L_b \times \left(\frac{2}{R_f}\right) \tag{2}$$

$$NM\ II: ln(S_b) = \ln(S_b^0) - \; S_b^0 L_b \times \left(\frac{2}{R_f S_b}\right) \tag{3}$$

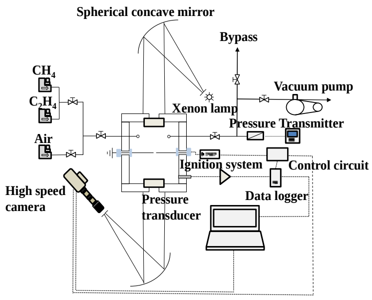

Figure 1. Schemaric diagram of the experimental setup.

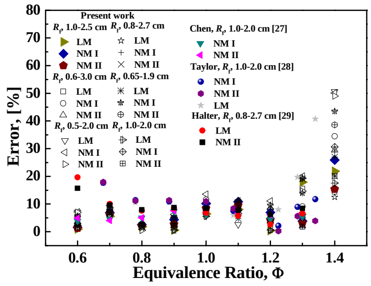

Figure 2. Error with experimental results as a function of equivalence ratio in CH_4-air at P_u = 1 atm.

The LM can be used for the spherical flame thickness assumed to be infinitesimally thin, weakly stretched and The NM I can be also valid for outwardly spherical flame propagating along with thermal expansion at large flame radius [9, 10]. Then the L_b and S_b^0 can be determined by the linear relationship of S_b and $2/R_f$, and such a nonlinear stretch effect in S_u^0 was analyzed by Frank and Sivashinsky [11]. The NM II was derived for quasisteady, adiabatic flame condition using an asymptotic method [12, 13], and its capability in predicting S_u^0 was investigated by the previous studies [14]. In Fig. 2, the error was also defined the difference of S_u^0 measured by varying R_f for the three extrapolation models from that calculated with GRI v 3.0. The error with LM in increase of ϕ increased in fuel-rich conditions. Resultantly, the results indicated that the error in S_u^0 measured with NM II was reduced significantly even at fuel-rich conditions. However, at fuel-rich conditions, further investigation could be required to clarify the sensitivity of flame radius to S_u^0. The current study also investigated them with several flame radii and the three extrapolation models (LM and NMs I and II). Similarly to the above results [15, 16], the error from all ranges of taken differently is not sensitive so much at 0.6 1.0. Resultantly, S_u^0 is best-fitted when the NM II is used at 10-25 mm. In the present study, the NM II and 10-25 mm were adopted for further study of CH_4/C_2H_4/air premixed flames. In the foregoing section, the extrapolation method and the range of flame radius in measuring S_u^0 were evaluated in methane-air premixed flame because of lack of experimental data on S_u^0 in CH_4/C_2H_4/air premixed flames. Using the NM II and 10-25 mm taken in the previous section, S_u^0 was measured for various ambient pressures and equivalence ratios in CH_4/C_2H_4/air premixed flames. Three Detailed chemistries (GRI v-3.0 [17], USC Mech II [18] and Sung Mech [19]) were compared to attain the priority in CH_4/C_2H_4-air flames. Figure 3 (a) compares experimental and numerical unstretched laminar at various equivalence ratios in CH_4/C_2H_4/air premixed flames. Numerical results with the three detailed chemisties were calculated

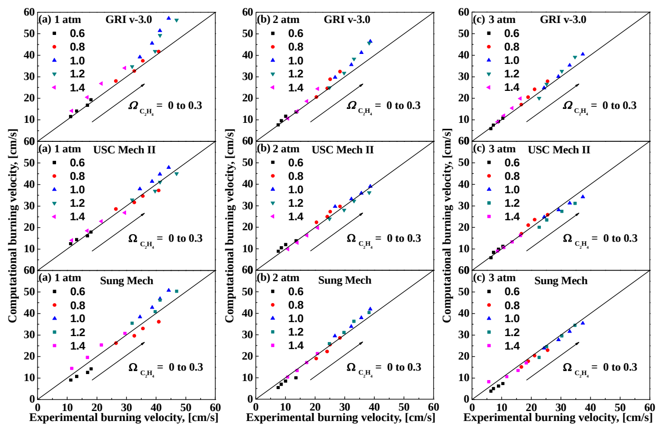

Figure 3. Comparison of Laminar burning velocities between eaperiment and calculation with cariation of detiled mehanims at 1 (a), 2 (b), and 3 (c) atm.

with PREMIX code [20]. The USC mech II in Fig. 6 is evenly distributed near linear line regardless of equivalence ratio and additional ethylene volume fraction to mixture, whereas in cases of GRI v 3.0, the discrepancy between experimental and numerical burning velocity increase with increasing additional ethylene volume fraction. Sung mechanism exhibits stark difference particularly at 1 atm. The average error in simulation value with USC mech II, in comparison with experimental data, is measured to 4.94 %. Sung mech is rather more matched to experimental flame speeds with increasing initial pressure. The error with GRI v–3.0 also increases with increasing ethylene volume fraction regardless of initial pressures. Resultantly, USC mech II describes 1-D expanding spherical flame speeds well in methane/ethylene-air premixed flames, in that the average error of simulation flame speeds with USC mech II is less than 6.63 %.

The cellular instability in premixed flames results in local flame acceleration due to buoyancy-induced, hydrodynamic, and diffusive-thermal effects. The hydrodynamic instability is well represented by the baroclinic torque term in vorticity equation. It is related to the density jump between burned and unburned mixture which is represend as $\sigma = (\rho_u / \rho_b)$ and characteristic flame thickness is defined as $l_f = (\lambda/C_p)/\rho_u S_u^0$. Another factor is the diffusive-thermal instability attributed to unbalance between mass and thermal diffusivity. Figure 4 shows sequential images of expanding spherical flames at 2, 3, and 4 atm at various ethylene volume fractions. Effective Lewis number, thermal expansion ratio, and flame thickness are indicated at the bottom of each photos. At 3 and 4 atm, the flame surface remains smooth at early stages, and then some cracks occur and branch until cells become uniform over the entire flame surface, even if the effective Lewis numbers is larger than unity. Therefore, propensity to destabilize the flame was not affected by the diffusive-thermal instability but by the hydrodynamic instability which relates to the thermal expansion ratio, and the flame thickness. This instability would be promoted because of the significant decrease in flame thickness and increase in thermal expansion ratio with increasing initial pressure and ethylene volume fraction. However, the effect of additional ethylene volume fraction is less influential in cells formation at the same pressure Thus, further onset of cellular instabilities was investigated through evaluating the critical Peclet number. And also the instability due to the substantial decrease of the flame thickness and increase of the thermal expansion ratio. Theory applied here accounts for both hydrodynamic and diffusive-thermal instabilities which are amalgamating the dependency of temperature transport coefficient. A theoretical analysis of the onset of instability in a spherically expanding flame was represented in [21, 22], where a hydrodynamic instability with Markstein correction was considered. The disturbed flame front can be written in the form $r = R_f\,(t)[1 + A(t)S_n(\theta, \phi)]$ [32], where $A(t)$ is the amplitude of the disturbance and S_n is the spherical surface harmonics with n as an integer. As the flame is expanded, the rate of growth of the relative amplitude of a disturbance of wavenumber n is given as follows in eq (4). The coefficient depends on the thermal expansion ratio, the Prandtl number Pr, and the wavenumber n. Definitions for ω_{DL} and Ω are given in [21, 22]. Figure 5 compares experimental and theoretical critical flame radii against ethylene volume. The experimental critical radius is defined at the moment when the burning velocity increased appreciably and lost the linear relationship between S_b and K, and theoretical one

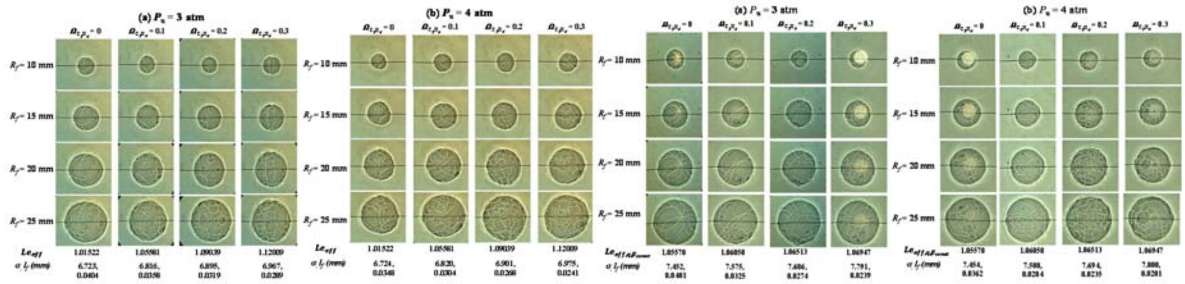

$\phi = 0.8$ $\phi = 1.2$

Figure 4. Effects of ethylene addition in CH4/air premixed flame on cellular instability at 3 (a) and 4 (b) atm.

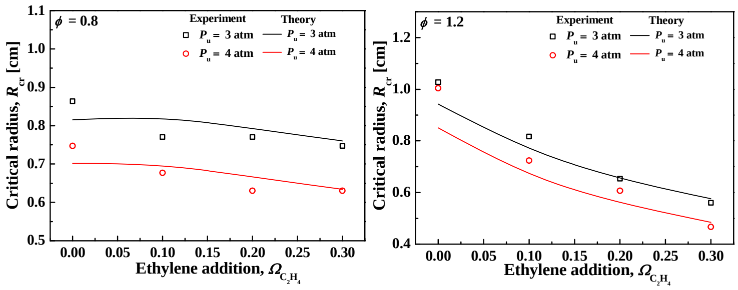

Figure 5. Mesured and theoretical critical radius with various mxing ratio and elevated pressure

$$\frac{1}{A}\frac{dA}{dt} = \frac{\dot{R}_f}{R_f}\left\{\omega_{DL} - \frac{l_f}{R_f}\Omega\right\}. \tag{4}$$

is shown in eq (4). As shown in Fig. 5, in both lean and rich conditions, experimental and theoretical critical radii decrease with increase in additional ethylene volume fraction and initial pressure. This means that the flame instabilities were promoted due to increase in thermal expansion ratio and decrease in flame thickness. However, in case of fuel-lean conditions, both experimental and theoretical critical radii slightly decreases and then have nearly constant with additional ethylene volume fraction regardless of decrease in flame thickness and increase in thermal expansion ratio. It was noted increasing effective Lewqis number results in slight decrease in flame radius, despite reduction of flame thickness and increase in thermal expansion ratio. Consequently, measured and theoretical critical flame radii shows excellent agreement.

Acknowledgement

This research was supported by Basic Science Research Program through the National Research Foundation of Korea (NRF) founded by the Ministry of Education (2016R1D1A1A02937106)

References

[1] Shy SS, Chen YC, Liu CC, Huang CM (2008). Experimental and numerical investigation of the effect of H_2 enrichment on laminar methane-air flame thickness. Combust Flame. 153: 510.
[2] Kim JS, Park J, Kwon OB, Lee EJ, Yun JH, Keel SI (2008). Preferential diffusion effects in opposed-flow diffusion flame with blended fuels of CH4 and H2. Int J Hydrogen Energy 33:842.
[3] Coppens FHV, Ruyck DJ, Konnov AA (2007). The effects of composition on burning velocity and nitric oxide formation in laminar premixed flames of $CH_4 + H_2 + O_2 + N_2$. Combust Flame 149:409.
[4] Scott J (2014). http://www.americanchemistry.com/Media/PressReleasesTranscripts/ACC-news-releases/US -Chemical-Invest ment-Linked-to-Shale-Gas-Reaches-100-Billion.html. American Chemical Council February.
[5] Fotache CG, Kreutz TG, Law CK (1997). Ignition of counterflowing methane versus heated air under reduced and elevated pressures. Combust Flame. 108:442.
[6] Davis SG, Law CK (1998). Determination of and fuel structure effects on laminar flame speeds of C_1 to C_8 hydrocarbons. Combust Sci Technol 140:427.
[7] Chen Z, Qin X, Ju Y, Zhao Z, Chaos M, Dryer FL (2007). High temperature ignition and combustion enhancement by dimethyl ether addition to methane-air mixtures. Proc Combust Flame. 31:1215.

[8] Chen Z (2015). On the accuracy of laminar flame speeds measured from outwardly propagating spherical flames: Methane/air at normal temperature and pressures. Combust Flame. 162: 2442.
[9] Burke MP, Chen Z, Ju Y, Dryer FL (2009). Combust. Effect of cylindrical confinement on the determination of laminar flame speeds using outwardly propagating flames. Combust Flame. 156:771.
[10] Ai Y, Zhou Z, chen Z, Kong W (2014). Laminar flame speed and Markstein length of syngas at normal and elevated pressures and temperatures. Fuel 137:339.
[11] Markstein GH (1951). Experimental and theoretical studies of flame-front stability. J Aeronaut Sci 18:199.
[12] Chen Z (2011), On the extraction of laminar flame speed and Markstein length from outwardly propagating spherical flames. Combust Flame 158:291-300.
[13] Ronney PD, Sivashinsky GI (1989). A theoretical study of propagation and extinction of nonsteady spherical flame fronts. SIAM J Appl Math 49:1029.
[14] Kelley AP, Law CK (2009). Nonlinear effects in the extraction of laminar flame speeds from expanding spherical flames. Combust Flame.156:1844.
[15] Rozenchan G, Zhu DL, Law CK, Tse SD (2003). Outward propagation, burning velocities, and chemical effects of methane flames up to 60 ATM. Proc Combust Inst. 29:1461.
[16] Halter F, Chauveau C, Djebaili-Chaumeix N, Gokalp I (2005). Characterization of the effects of pressure and hydrogen concentration on laminar burning velocities of methane-hydrogen-air mixtures. Proc Combust Inst 30:201.
[17] Smith GP et al, GRI-MECH 3.0 < http://www.me.berkeley.edu/gri_mech/>.
[18] Wang H, You X, Joshi AV, Davis SG, Salkin A, Egolfopoukos F, Law CK, USC MECH II <http://ignis.use.edu/USC_II.htm>.
[19] Sung CJ, Li B, Law CK, Wang H. Wang MECH < https://www.princeton.edu/~cklaw/kinetics/slw001/index.html>.
[20] Kee RJ, Grcar JF, Smooke MD, Miller JA (1985). A Program for modeling steady, laminar, one-dimensional premixed flames. Sandia National Laboratory Report SAND85-8240.
[21] Matalon M (2007). Intrinsic flame instabilities in premixed and nonpremixed combustion. Annu Rev Fluid Mech. 39:163.
[22] Addabbo R, Bechtold JK, Matalon M (2002). Wrinkling of spherical expanding flames. Proc Combust Int. 29:1527.